RESEARCH PAPER

Design and Development of a Prosthetic Leg for People with Transfemoral Amputation Consisting of a Polycentric Knee Machined by Multi-Axis CNC and a Socket-Liner System with Simple Mechanical Adjustment

Miguel Angel Escobar Guachambala[1*], Ember Geovanny Zumba Novay[2], Edwin Rodolfo Pozo Safla[3], Jorge Sebastián Buñay Guamán[4], Luis Santiago Choto Chariguamán[5]

[1*]Ingeniero Mecánico - Magister En Diseño Producción Y Automatización Industrial, Escuela Superior Politecnica de Chimborazo (ESPOCH). ORCID: https://orcid.org/0000-0002-9683-1479.

Email: maescobar@espoch.edu.ec (Corresponding Author)

[2]Ingeniero de Mantenimiento - Ingeniero en Administración y Producción Industrial - Magister en Diseño Industrial y de Procesos, Universidad Nacional Mayor de San Marcos (UNMSM). ORCID: https://orcid.org/0000-0002-2121-8418.

Email: ember.zumban@unmsm.edu.pe

[3]Ingeniero Mecánico - Magister en Diseño, Producción y Automatización Industrial, Escuela Superior Politecnica de Chimborazo (ESPOCH). ORCID: https://orcid.org/0000-0002-8931-3577. Email: edwin.pozo@espoch.edu.ec

[4]Ingeniero Mecánico - Magister en Ingeniería Matemática y Computación, Escuela Superior Politecnica de Chimborazo (ESPOCH). ORCID: https://orcid.org/0000-0002-8931-3577. Email: jorge.bunay@espoch.edu.ec

[5]Ingeniero de Automotriz - Magister en Manufactura y Diseño Asistido por Computador, Escuela Superior Politecnica de Chimborazo (ESPOCH). ORCID: https://orcid.org/0000-0003-2499-3337. Email: lchoto@espoch.edu.ec

ABSTRACT

This study presents the design, simulation, and manufacturing of a transfemoral prosthetic knee based on a polycentric four-bar linkage mechanism, aimed at achieving an optimal balance between biomechanical performance, structural reliability, and cost-efficiency. The system was fabricated using 5-axis CNC machining, demonstrating its feasibility as a robust alternative to additive manufacturing for load-bearing biomedical components. Structural performance was evaluated through finite element analysis (FEM) under loading conditions defined by ISO 10328. Results indicate that the prosthesis operates within safe mechanical limits, with maximum stresses significantly below the yield strength of the selected materials and safety factors exceeding critical thresholds in both static and dynamic scenarios. Maximum deformation values remained below 2.5 mm under worst-case conditions, ensuring compliance with international standards and preserving functional integrity during the gait cycle. Fatigue analysis revealed that critical components exceed 10^8 cycles, confirming high durability and long-term operational viability. From a biomechanical perspective, the polycentric mechanism reproduces a physiologically consistent motion trajectory, enabling a functional range of motion between 90° and 180°. The integration of a spring-based return mechanism improves energy efficiency during gait by facilitating energy storage and release without increasing system complexity. Additionally, the offset configuration of the upper connector enhances the moment arm, contributing to smoother limb advancement and a more natural walking pattern. A key innovation lies in the implementation of a fully mechanical socket-liner coupling system based on threaded

*Author for Correspondence: smaescobar@espoch.edu.ec

adjustment, eliminating the need for costly imported technologies such as pin-lock or vacuum systems. This significantly reduces production and maintenance costs, making the solution suitable for low- and middle-income regions. Overall, this work provides a technically validated, economically viable, and scalable prosthetic solution, contributing to advancements in prosthetic knee design and improving accessibility for transfemoral amputees.

Keywords: Prosthesis, four-bar linkage, polycentric knee, static analysis, machining process

How to cite this article: Guachambala MAE, Novay EGZ, Safla ERP, Guamán JSB, Chariguamán LSC. Design and Development of a Prosthetic Leg for People with Transfemoral Amputation Consisting of a Polycentric Knee Machined by Multi-Axis CNC and a Socket-Liner System with Simple Mechanical Adjustment. Int J Drug Deliv Technol. 2026;16(22s): 75-91. DOI: 10.25258/ijddt.16.22s.9

Source of support: Nil.

Conflict of interest: None

1. Introduction

Previous studies have developed passive 6-bar linkage systems for transfemoral amputees, considering the connections formed between the 4-bar linkage knee mechanism and the ankle-foot system [1]. The sizing of the 4-bar linkage mechanism to generate the characteristic poleoid has also been performed, and the validity of the prototype's strength was verified using the finite element method with 7075 T6 aluminum [2]. Furthermore, commercial models already exist with dimensions that provide good stability, but these can always be optimized using iterative algorithms until no further iterations are possible, thus improving their functionality [3]. Another study focuses entirely on the design and selection of the most suitable damping system for a 4-bar linkage knee prototype [4]. It has been identified that the biggest problem with passive systems is that they require a lot of metabolic energy from the patient; for this reason, an active system is sometimes chosen [5]. There are knee mechanisms based on mechanical gear transmission that allow for excellent control of the instantaneous center of rotation [6]. Systems based on rotary cylinders together with a rotary piston are also efficient but more sophisticated [7].To validate the correct prototype design, it is necessary to use the ISO 10328 standard for conditions I and II. Condition I corresponds to the initial contact phase, while Condition II corresponds to the lift-off phase. It is important to note that the stress values obtained must be less than the material's elastic limit, and the fatigue safety factor must be greater than 1 [8]. This standard establishes certain levels depending on the patient's body weight. Level P4 corresponds to patients up to 80 kg, where a static load of 4130 N is applied [9]. For weights up to 65 kg, P3 is used, with a load of 1610 N for condition I and 1395 N for condition II [10]. The deformation value obtained for a P4 load must be less than 2.5 mm, and the maximum stresses must be less than the material's yield strength [11]. In the fatigue or cyclic loading test, it is important that the prototype has a lifetime of $10x10^6$ [12]. A deformation of up to 5 mm is also possible [13].The sizing of the 4-bar linkage system is important because the instantaneous center of rotation (ICR) must generate a curve similar to that of the human knee [14]. In another study, a prototype was developed that showed a 15% to 18% error in the angle curve with respect to the percentage of the gait cycle [15].The materials used for manufacturing knee mechanisms are varied, but currently, additive manufacturing and carbon fiber are preferred [16]. Additive manufacturing is commonly used to reduce the cost of the prototype [17]. When conventional machining is used, aluminum alloys such as 7075 or 6061 are preferred because they yield acceptable safety factor values [18].

The damping or quick-return system for knee prostheses can be entirely mechanical, using springs or pneumatics [19]. Hydraulic cylinders are also commonly used, although the control system is more complex, and therefore the cost of the prototype increases [20]. The most advanced systems contain force sensors and inertial sensors to control the hydraulic cylinders via microcontrollers [21]. Hybrid systems controlled by electromagnetism improve the results in knee flexion angle curves [22]. Certain control systems use actuators such as small electric motors where the knee flexion and extension angle can be controlled depending on different movements performed by the user [23].

Simulation validation of the prototype for a gait cycle can be performed using a prosthetic test platform where joint movement is controlled by linear actuators and mo-

tors [24]. Humanoid bipedal models controlled by actuators can also be generated, where they walk on a completely flat surface [25]. In more complex systems, mathematical models accompanied by programming can be used [26]. Similarly, it is possible to perform a dynamic analysis of stress behavior in real time throughout the gait cycle using FEM simulation [27]. Another alternative is to analyze the entire bipedal model through a static analysis for each phase of the gait cycle separately [28].

Socket design is also necessary for proper adaptation to the knee prototype, where performing the analysis using the finite element method presents a significant challenge due to the nonlinear system that must be modeled [29]. Generally, specialized laboratories carry out tests for the validation of transfemoral and transtibial sockets according to ISO 10328 standards [30]. The socket design process begins with reverse engineering, followed by the application of the finite element method to verify its validity and subsequent construction [31].

The objective of this study is to utilize 5-axis CNC technology to create a prototype polycentric knee for patients with transfemoral amputations. This method will enable the production of more organic or complex geometries that would otherwise be time-consuming to manufacture using traditional machining techniques, thereby enhancing both appearance and aesthetics. The findings are expected to decrease reliance on technologies such as additive manufacturing and broaden the options for producing knee prostheses. Additionally, the goal is to implement a fully mechanical adjustment mechanism that uses threading between the liner and the socket, eliminating the need to import costly systems like Pinlock or active vacuum systems, which will help lower the prototype's cost. Although the prototype is designed for an adult, the length of the prosthetic tube can be adjusted to suit patients of varying heights.

2. Materials and Methods

2.1. Dimensioning of the 4-bar linkage

The dimensions of the four-bar linkage were determined through a literature review, as the primary objective was to implement five-axis CNC machining and fabricate the prototype in either aluminum or steel. The overall dimensions are as follows: link AB 89.53 mm, link BC 35.49 mm, link CD 78.92 mm, and link AD 58.75 mm [32]. The coupler is positioned 13.78 mm above link BC and 13.72 mm perpendicular to link BC, as shown in Figure 1.

Figure 1. Dimensions of the 4-bar linkage knee prototype. (a) Overall dimensions where AB link is 89.53 mm, BC link is 35.49 mm, CD link is 78.92 mm, and the AD bed is 58.75 mm with an angle formed with the horizontal of 29.93°; (b) Poloid generated by the coupler of the 4-bar linkage

2.1.1. Initial model

The impulse force generated by the patient's gait causes the coupler to move, compressing the spring, which then returns to its original position after storing energy, before the patient makes initial contact between the heel and the surface.

Figure 2. Curves generated by the 4-bar linkage and the complete leg model: (a) Coupler curve generated by the coupler point of the 4-bar linkage. (b) Curve generated during the swing phase. (c) Curve generated when the patient moves from sitting to standing. (d) Curve generated during the initial swing phase, as well as the proper compression of the spring.

2.2. Prototype design of a prosthetic leg

The prototype prosthetic leg is shown in Figure 3.

a) The prosthetic leg is shown at 90°, representing the patient's seated position, while Figure 3

b) shows the leg as the patient begins to stand up, reaching 180°, which is when the patient is in an upright position.

(a) **(b)** **(c)**

(d) **(e)**

Figure 3. Prosthetic leg mobility. (a) Prototype leg at its maximum flexion of 40°; (b) Prosthetic leg prototype at 90°; (c) Prosthetic leg prototype at 130°; (d) Prosthetic leg prototype at 160°; (e) Prosthetic leg prototype at 180°.

The complete prosthetic leg assembly is shown in Figure 4a, which is divided into 5 subsystems as shown in Figure 4b, where there is a total of 38 elements shown in Figure 4c. Subassemblies 1 and 2 are assembled together with subassembly 3 using set screws, as shown in Figure 4d), and finally, subassembly 5 is assembled by pressure and adjustment using the mechanism shown in Figure 4e. The socket-liner system consists of 4 elements as shown in Figure 4f), where element A must be screwed onto the silicone liner, then inserted into element C, and this is adjusted to the socket by means of element B.

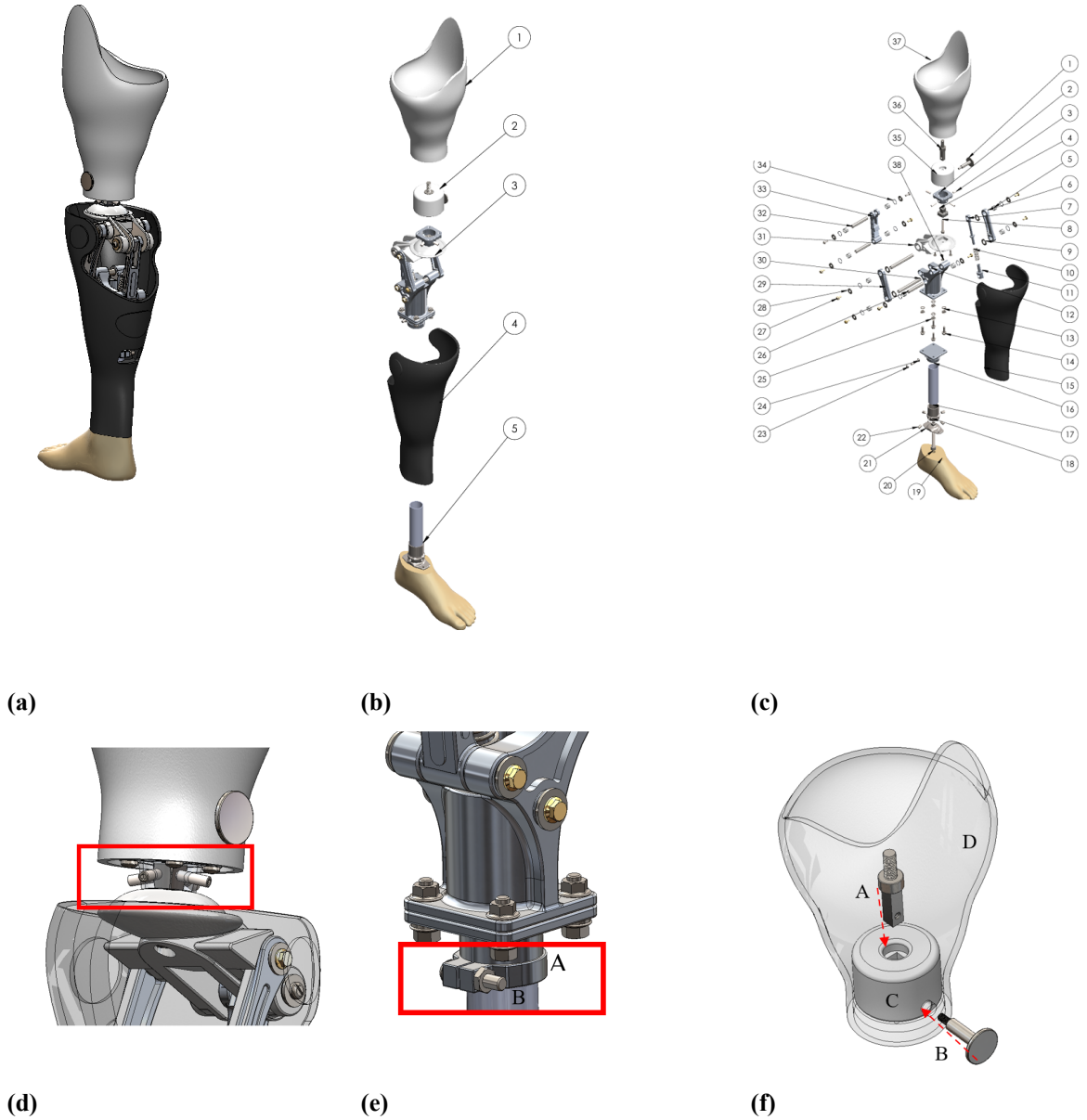

Figure 4. Adjustment and joining modes of the prosthetic leg systems: (a) Fully assembled prosthetic leg prototype; (b) Prosthetic leg prototype divided into 5 subsystems; (c) Exploded view of the CAD model with 38 elements in total; (d) Joining mechanism of the polycentric knee to systems 1 and 2; (e) Adjustment mechanism of the polycentric knee to system 5. (f) Adjustment and joining mechanism of the socket-liner system.

2.3. Selection of the material for machining the links of the polycentric knee

.

Material selection is crucial to ensure the prototype is both lightweight and strong. Therefore, material selection software is used. The price is limited to $10 per kilogram, and the following parameters are entered: an approximate density ranging from 1700 kg/m³ to 3000 kg/m³, a modulus of elasticity of 60 GPa, and a yield strength of 235 MPa. Finally, the ultimate tensile strength is set at 250 MPa. A further restriction is applied to limit the material's corrosiveness. Using Ashby's method, the total number of materials is reduced to just two options: 7075 T6 aluminum and 6061 T6 aluminum

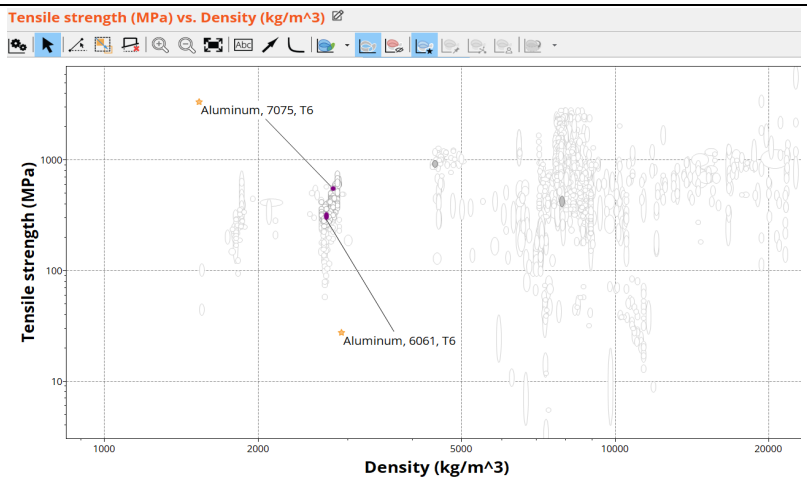

Figure 5. Pre-selected materials for machining the main links of the prototype: Aluminum 7075 T6 and Aluminum 6061 T6

holes is of the "no separation" type because the shaft needs to rotate but not slide axially. The connection between the upper link and the connector is of the "bonded" type since the fastening elements prevent movement and rotation on all axes, as shown in Figure 6a. The connection between the side links with respect to the upper and lower links is of the no-separation type, as shown in Figure 6d). Finally, the connection between the outer edge of the bearings and the holes is also of the no-separation type, as shown in Figure 6b). After applying various mesh processing tools, the mesh quality improved significantly, reaching an average of 0.79 according to the element quality metric, as shown in Figure 6h. To achieve a good mesh quality, tetrahedral and hexahedral elements were used in the most complex elements and with an element size of 3 mm. In this way, it can be observed that the elements with the lowest mesh quality are the lower and upper links.

2.4. Parameters and conditions entered for static and dynamic simulation

The simulation is divided into three parts. The first part considers only the knee prosthesis. The second part covers the lower system, consisting of the tube and the prosthetic foot. Finally, the upper components, comprising the socket and locking elements, are included. For material allocation, 7075 T6 aluminum was chosen for all machinable components due to its tensile strength of approximately 572 MPa, compared to approximately 310 MPa for 6061 T6 aluminum. PETG, with an ultimate strength of 70 MPa, was used for the upper link. AISI 1018 steel, with a Young's modulus of 370 MPa and an ultimate strength of approximately 440 MPa, was selected for the five axes. Finally, the material assigned to the bearings is AISI 52100 chromium alloy steel with an ultimate strength of 400 MPa and a Young's modulus of 250 MPa.

The assignment of contact types is performed element by element. The contact between the shafts and the bearing

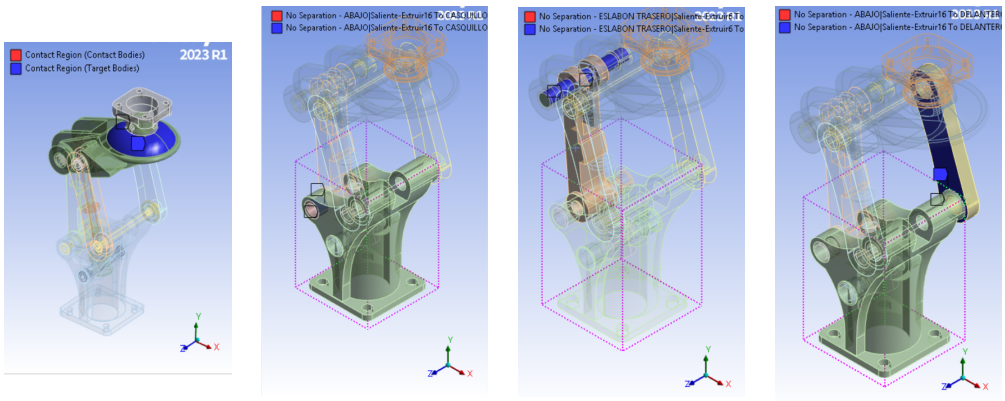

(a) **(b)** **(c)** **(d)**

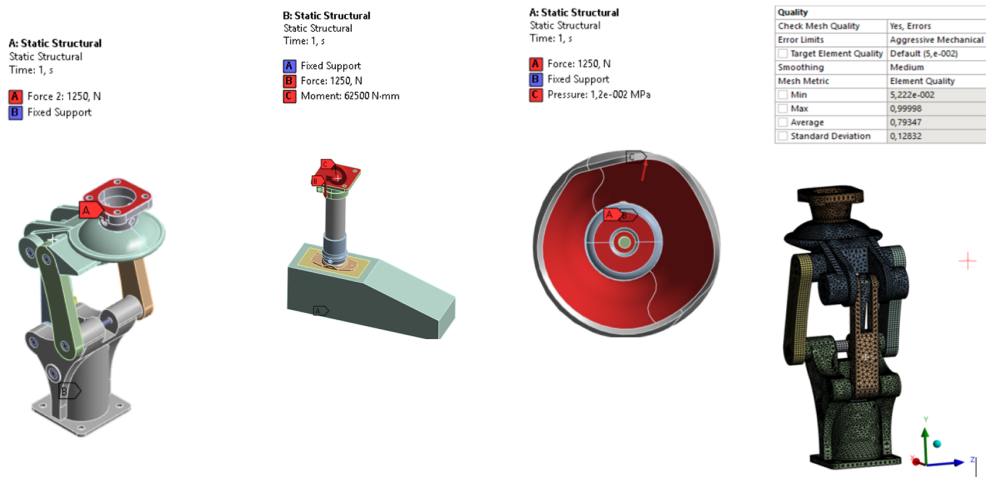

(e) **(f)** **(g)** **(h)**

Figure 6. Creation of contacts and assignment of loads along with boundary constraints. (a) Between the upper link and connector of the knee and socket system; (b) Contact between bearings and holes; (c) Contact between shafts and holes; (d) Contact between side links and the lower element; (e) Loads and constraints entered for the knee prototype simulation; (f) Loads and constraints assigned on the lower system; (g) Loads and constraints assigned on the upper system; (h) Mesh quality of the knee prototype (0.793).

For static and dynamic simulation during the most critical phase of the gait cycle, i.e., when the patient places the entire sole on the ground (at that moment, the patient's full body weight is borne), a negative vertical load of 1250 N is applied to the upper connection between the knee and the socket. The boundary condition is assigned to the lower part of the prosthesis; this is a fixed support that prevents translation and rotation on all axes, as shown in Figure 6e. For cyclic loading simulation, a table is created with the values that make up the S-N curve for all the materials involved, a fluctuating load of 1250 N is applied, and the Goodman criterion is selected. For the second part of the simulation, the load corresponding to the patient's body weight multiplied by a safety factor of 1.8 is assigned, as well as the moment of 62,500 N·mm around the z-axis in a negative direction due to the force applied to the upper link being transferred to the lower connector, as shown in Figure 6f. The connector between the prototype and the prosthetic tube is assigned to the material 7075 T6 aluminum; the prosthetic tube is aluminum, and both connectors are made of AISI 1018 steel. For the third and final part of the simulation, a force of 1250 N is assigned to the upper face of the connecting element, and a pressure of 0.12 MPa is applied, representing the pressure exerted by the stump on the socket's inner face. It should be noted that this pressure is normal to the entire surface, as shown in Figure 6g).

FEM validation is also performed using ISO 10328 standards, following the loads, distances and restrictions indicated therein.

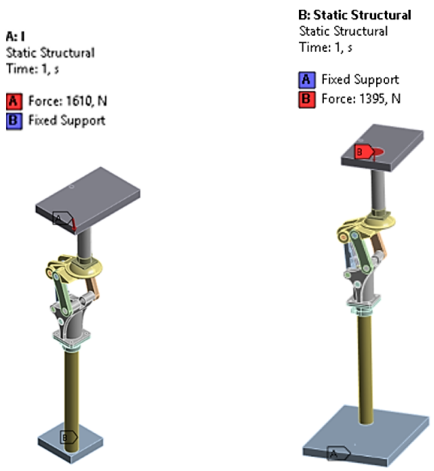

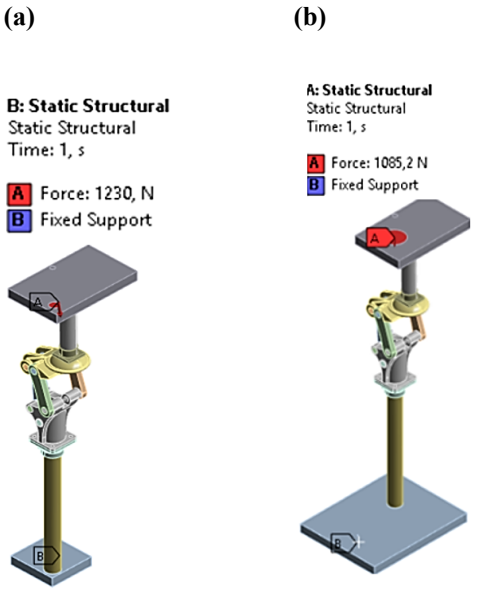

Figure 7. Loads and restrictions assigned for static and dynamic simulations according to ISO 10328: (a) Load applied under condition I to static load; (b) Load applied under condition II to static load; (c) Load applied under condition I to dynamic load; (d) Load applied under condition II to dynamic load.

2.5. Parameters and conditions entered for spring validation

The spring is helical with 11 active coils and a spring rate of 8 N/mm with a wire diameter of 2 mm. The material assigned to the spring for the purpose of determining the safety factor during the swing phase is A228 steel with an ultimate strength of 2100 MPa and a Young's modulus of 1770 MPa.

2.6. Prototype validation for a gait cycle using a bipedal model

The prototype's functionality is validated using a bipedal model representing the tibia, femur, and knee of both legs. Rotational connections are created for all axes and bearings, while translational joints are assigned to the spring guide. The aluminum components have a Young's modulus of 7.17 x 10^4 MPa, a density of 2.74 x 10^{-6} kg/mm³, and a Poisson's coefficient of 0.33. Contact between the foot model and the surfaces is established, resulting in a stiffness of 5 x 10^5 and a damping coefficient of 200 N·s/m, along with static and dynamic friction coefficients of 0.8 and 0.3, respectively. Finally, a friction change rate of 4 mm/s is added, and the rate at which the dynamic friction reaches its maximum value is 0.08 mm/s. A simulation time of 2 seconds is performed because, through iterations, it is verified that it more closely resembles reality, as shown in Figure 8.

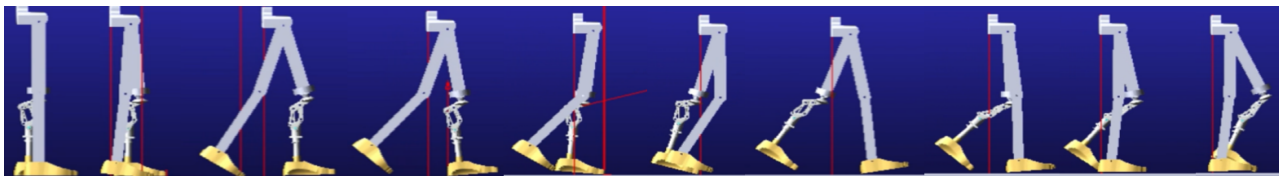

(a)

Figure 8. Virtual simulation for a walking cycle.

2.7. Machine configuration for 5-axis CNC machining

The machine selected for machining is the HY 3040 5-axis model. Once each element is inserted, it is properly oriented on the machine table, and the MSC coordinate system is defined, where the origin is the center of the material and the z-axis is perpendicular to the table where it is located. The selected cutting speed is 200 m/min with a feed per tooth of 0.2. The milling cutters to be used are 3 mm and 9 mm in diameter, with a 10 mm and 12 mm drill bit and a 6 mm ball end mill for all elements, as shown in Figure 9.

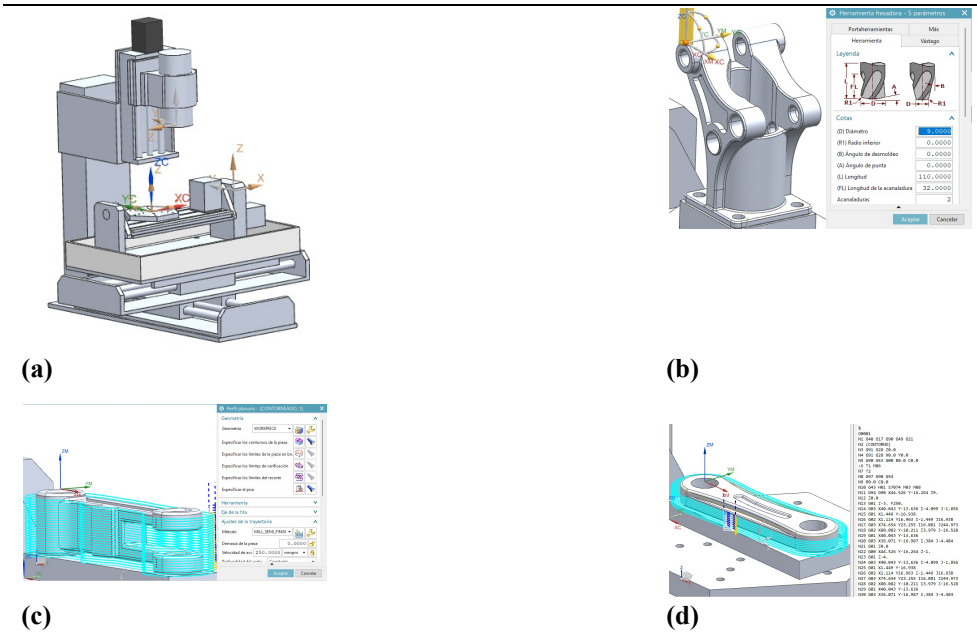

Figure 9. Virtual configurations and simulations of some elements prior to machining on the HY 3040 machine: (a) CAD model of the HY 3040 5-axis CNC machine; (b) Creation and configuration of tools for machining the lower link; (c) Trajectory simulation for the drive link; (d) Virtual simulation and generation of codes for the front links.

3. Results

3.1. Results of static and dynamic analysis using the finite element method

3.1.1. Results of static analysis using the finite element method

The maximum deformation during the full support phase is 0.75 mm, occurring in the upper connecting element, while the maximum stress is 57.107 MPa, generated in the side bars due to contact with the locking elements of the upper link at these points. These points also have the lowest static safety factor, which is 3.81. The maximum deformation under static load in condition I of the prototype is between 1 mm and 2.5 mm, while for condition II it is between 0.37 mm and 1.12 mm. The maximum stress under condition I is 108.84 MPa, while for condition II it is 129.3 MPa. Finally, the minimum safety factor under condition I is 5, while for condition II it is approximately 3 to 5, as shown in Figure 10.

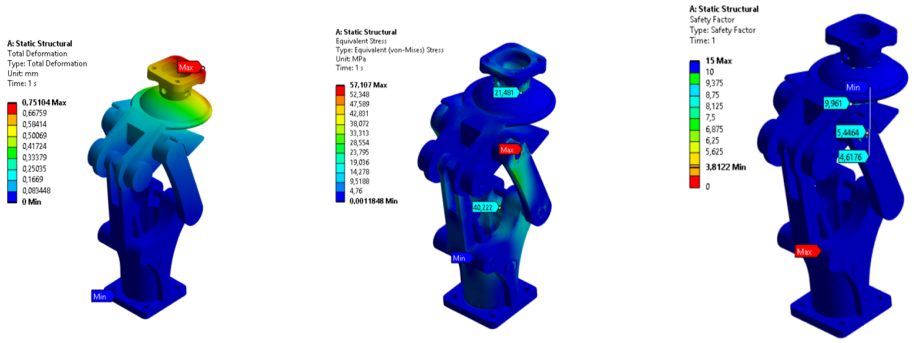

(a) **(b)** **(c)**

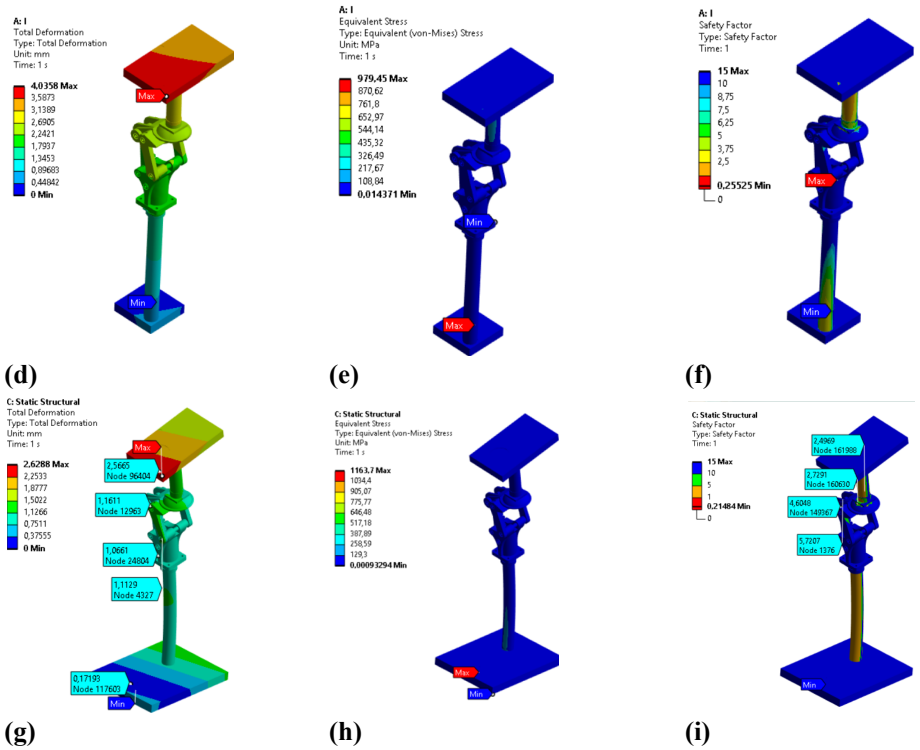

Figure 10. Results of the static simulation of the knee prototype. (a) Maximum deformation in stance phase (0.75 mm);
(b) Maximum stress in stance phase (570.107 MPa); (c) Minimum safety factor in stance phase (3.81); (d) Deformation under ISO 10328 condition I (1mm-2mm); (e) Stress under ISO 10328 condition I; (f) Minimum safety factor ISO 10328 condition I; (g) Deformation under ISO 10328 condition II; (h) Stress under ISO 10328 condition II; (i) minimum safety factor ISO 10328 condition II.

3.1.2. Dynamic analysis using the finite element method

The number of fatigue cycles during the support phase is 1 x 10^8 cycles, indicating a long service life, while the minimum safety factor is 2.54, indicating a correct design of the link dimensions and thicknesses. The maximum life under condition I is 1 x 10^{-6} cycles, as it is for condition II. The minimum safety factor under dynamic load is 4.5 for condition I and 5 for condition II, as shown in Figure 11.

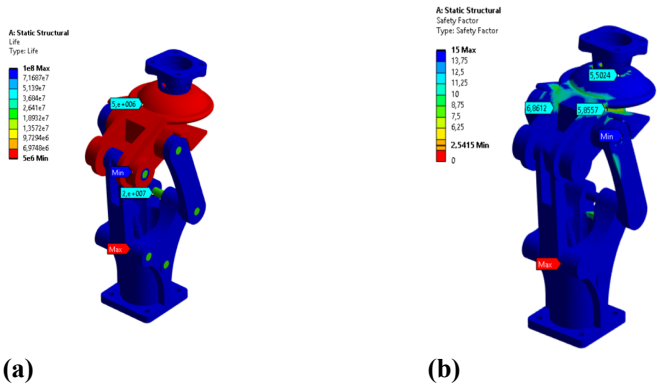

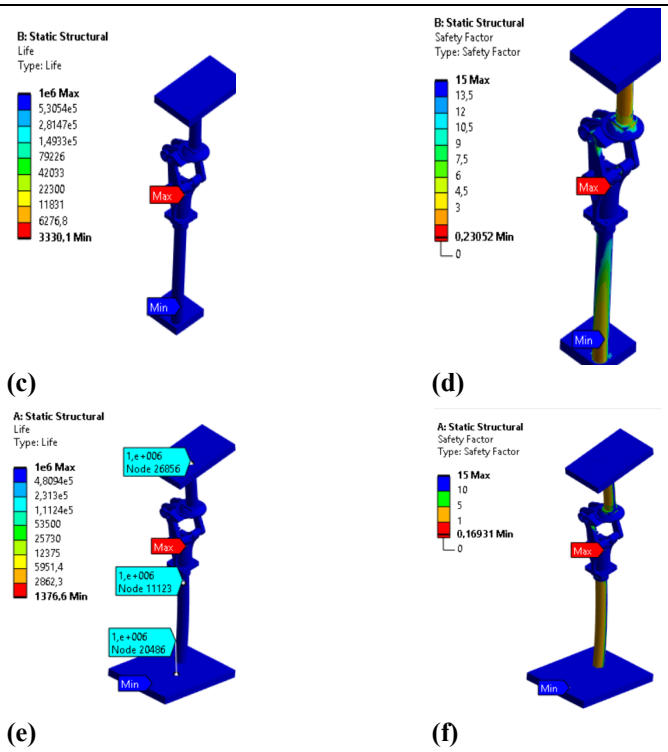

Figure 11. Results of the fatigue analysis of the knee prototype: (a) Number of cycles in the stance phase; (b) Minimum safety factor in the stance phase (2.54); (c) Number of cycles under ISO 10328 condition I. (d) Minimum safety factor under ISO 10328 condition I. (e) Number of cycles under ISO 10328 condition II; (f) minimum safety factor under ISO 10328 condition II.

3.2. Results of the dynamic analysis of the spring

The fatigue life for the spring is 1x10^11 cycles while the minimum safety factor is 1.31 as shown in figure 12.

Figure 12. Results of the spring fatigue simulation: (a) Number of cycles the spring will withstand under cyclic loading 1x10^11 cycles; (b) Minimum safety factor of the fatigue spring of 1.3166.

3.3. Results of the static and dynamic analysis of the lower and upper systems

The lower system, consisting of the foot and prosthetic tube, has a minimum static safety factor of 2.28, which occurs at the top of the tube where the greatest stress is concentrated. The socket has a static safety factor of 8.58 and a dynamic load of 3.576. The liner adjustment element has a minimum safety factor of 12.307, and the locking pin has a safety factor of 15, as shown in Figure 13.

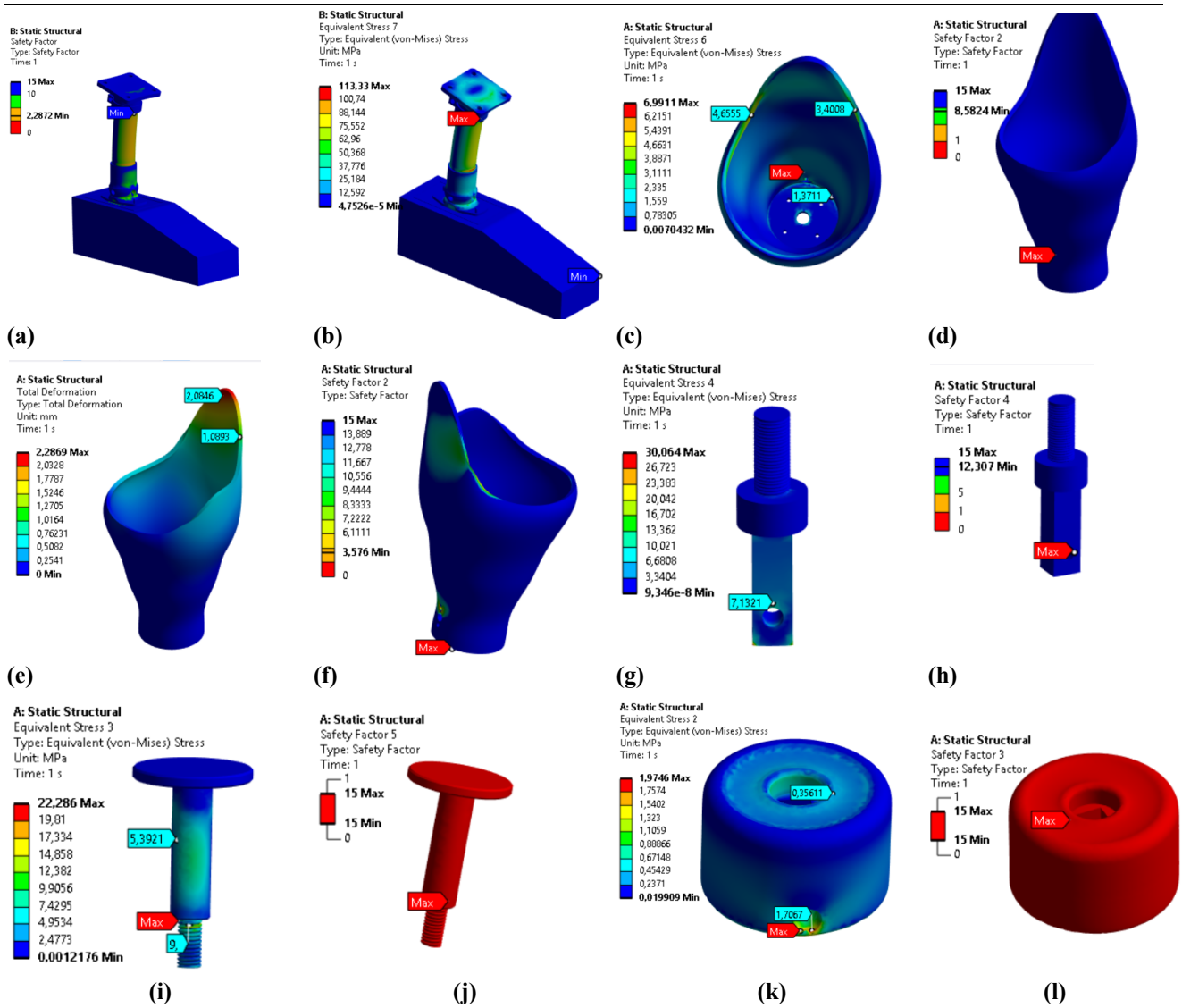

Figure 13. Results of the spring fatigue simulation: (a) Number of cycles the spring will withstand under cyclic loading: 1 x 10^11 cycles; (b) Minimum safety factor of the fatigue spring: 1.3166.

Figure 14 shows the position curve measured on the y-axis with respect to time.

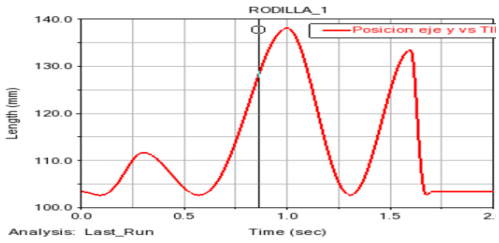

(a)

Figure 14. Results of the virtual simulation for a gait cycle: (a) Position curve on the "y" axis of the prosthetic knee with respect to time (Percentage of gait cycle).

3.4. Machined elements and final assembly of the prosthetic leg prototype

Figure 15 shows each of the parts machined using a 5-axis CNC. Figure 15a) corresponds to the bed link, Figure 15b) to the upper link or coupler along with the adjusting element, Figure 15c) to the rear element, and Figure 15d) to the element that acts as a spring guide. Figure 15e) corresponds to the front links, while Figure 15f) is the clamping element between

the bed and the tube. Finally, element 15c) corresponds to the spring support head, and Figure 15h) corresponds to the locking element.

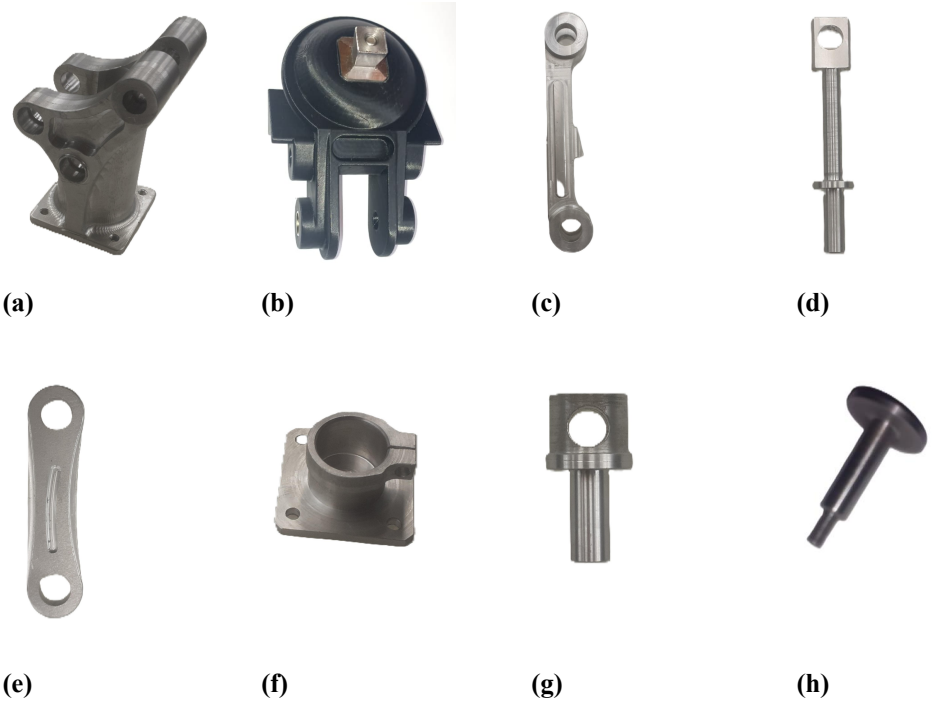

Figure 15. Components machined using multi-axis CNC technology: (a) Lower link or base; (b) Upper link or coupler made using additive manufacturing (black) and the element for attaching it to the socket system (gray); (c) Drive link; (d) Spring guide; (e) Follower link; (f) Element for coupling the knee prototype with the prosthetic tube; (g) Spring base where the guide enters; (h) Adjustment and locking element between the socket and the silicone liner.

Figure 16a) shows the assembly of each of the links and connections of the polycentric knee prototype machined from 7075 T6 aluminum. Figure 16b) shows the side view of the same, while Figure 16c) shows the assembly between the socket, the knee, and the foot.

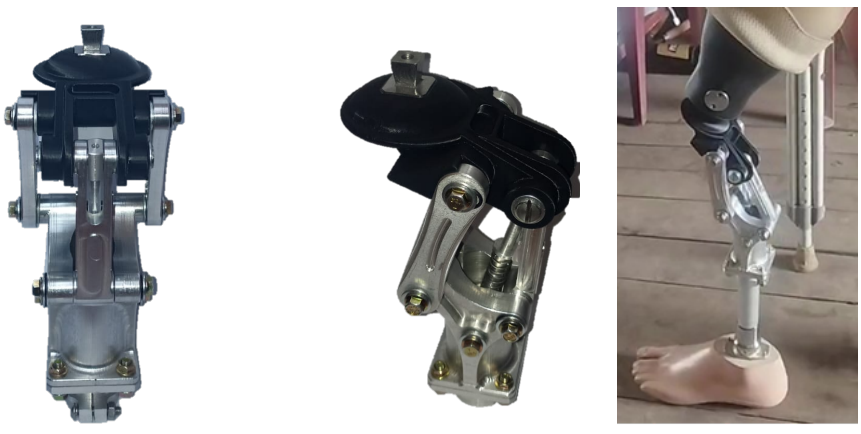

Figure 16. Figure 16a) shows the assembly of each of the links and connections of the polycentric knee prototype machined from 7075 T6 aluminum. Figure 16b) shows the side view of the polycentric knee prototype, while Figure 16c) illustrates the assembly of the socket, knee, and foot.

4. Discussion

The finite element method (FEM) validation using ISO 10328 for the knee mechanism resulted in deformation below the maximum allowed, complying with the standard, which is up to 5 mm [13]. While other studies have restricted the maximum deformation value to 2.5 mm, the prototype still meets the requirements, as the safety factor in both the static and dynamic analyses is greater than 1.5. The highest stress values are found in the upper element precisely because it is made of a material with a lower ultimate tensile strength than the other elements, but it still meets the required strength.

The prosthetic leg prototype has a range of motion from 90 to 180 degrees, although it can flex up to 30 degrees, which is not a common movement. However, if needed, the prototype can meet this requirement, as in [1]. The virtual simulation allowed us to obtain a curvature in a gait cycle, representing the variation in the position of the upper element along the y-axis with respect to time. This curvature can be likened to the knee flexion curvature shown in [33]. The socket was not used in the gait cycle simulation because it does not representatively influence the behavior of the polycentric knee.

In the design of the upper component, the connector is offset from the line of action of the prosthetic tube. This offset allows for greater momentum to lift the prosthesis and facilitate a smoother stride. The mechanical placement system, which uses threading between the socket and the liner, is basic and practical for the patient. The user only needs to tighten or loosen the locking element to position the entire prosthetic leg. This system offers the same ease of use as pin-lock, vacuum, cuff, and suspension sleeve systems, with the advantage of being more cost-effective and easier to manufacture in developing countries [34].

3.5. Future Work

Future improvements could include the application of a hydraulic or pneumatic piston to enhance gait fluidity, as well as a control system to improve the knee's characteristic poleloid. The prosthesis' efficiency should also be evaluated under real-world conditions through testing with transfemoral amputee patients. This will allow for a comparison of knee flexion and extension curves with those of healthy test subjects to determine their similarity, even though virtual simulation theoretically validated the prototype's efficiency.

3.6. Limitations

The upper link was not machined from aluminum because this would have compromised the prototype's weight for proper use by the patient. However, the safety factors from the static and dynamic analyses indicate adequate resistance in PETG material. Additionally, no tests were performed with a patient with a transfemoral amputation, as the focus of this study was to apply multi-axis CNC machining as an alternative for prosthesis fabrication.

5. Conclusions

The prototype exhibits adequate mechanical strength for individuals weighing up to 60 kg and provides the necessary flexion angle for comfortable use in both seated and standing positions. Additionally, it is important to highlight that multi-axis CNC machining technology represents an efficient alternative for the manufacturing of knee prostheses.

The results obtained in this study demonstrate that the proposed transfemoral prosthesis, based on a polycentric four-bar linkage mechanism and manufactured through 5-axis CNC machining, achieves a robust balance between mechanical performance, manufacturability, and cost-efficiency. From a structural standpoint, finite element method (FEM) analysis, validated under ISO 10328 standard conditions, confirms that the prototype operates within safe mechanical limits. The results show maximum stresses significantly below the yield strength of the selected materials and safety factors above critical thresholds under both static and dynamic loading conditions. This evidences a high level of structural reliability and suitability for real-world loading scenarios.

The observed deformation values (≤ 2.5 mm under critical conditions) ensure compliance with international standards while preserving functional integrity during the gait cycle. Fatigue analysis further reinforces the durability of the design, with lifetimes exceeding 10810^8108 cycles in critical components, indicating high long-term operational viability and reduced maintenance requirements. These results position the proposed design as a competitive alternative to existing prosthetic systems, particularly in terms of mechanical strength and resilience.

From a biomechanical perspective, the polycentric mechanism effectively reproduces a physiologically consistent motion trajectory, enabling a functional range of motion between 90° and 180°. The incorporation of a spring-based return mechanism contributes to energy storage and release during the gait cycle, improving movement efficiency without increasing system complexity. Additionally, the eccentric configuration of the upper connector increases the moment arm, facilitating smoother limb advancement and contributing to a more natural gait pattern.

A key innovation of this study lies in the implementation of a fully mechanical socket–liner coupling system based on threaded adjustment. This solution eliminates the need for costly imported technologies, such as pin-lock or vacuum systems, significantly reducing production and maintenance costs without compromising usability or adaptability. This aspect is particularly relevant for application in low- and middle-income countries, where accessibility and affordability are critical factors. The successful application of multi-axis CNC machining demonstrates its feasibility as an alternative to additive manufacturing in prosthetic fabrication. Unlike additive methods, CNC machining provides superior surface finish, higher dimensional accuracy, and better material homogeneity—key characteristics for load-bearing biomedical devices. This expands the range of available technological solutions for prosthetic development, especially in environments with established subtractive manufacturing capabilities.

However, despite the strong simulation-based validation, the absence of experimental testing with transfemoral amputee patients constitutes a limitation that should be addressed in future work. Clinical validation will be essential to evaluate gait symmetry, metabolic cost, user comfort, and long-term biomechanical adaptation. Furthermore, the integration of semi-active or active systems (such as hydraulic dampers or sensor-based control systems) could further enhance gait dynamics and adaptability across different terrains.

This research provides a technically validated, economically viable, and manufacturable prosthetic solution aligned with the requirements of high-impact biomedical engineering research. It not only advances the state of the art in knee prosthesis design but also offers a scalable framework for future innovations aimed at improving mobility and quality of life for transfemoral amputees, particularly in resource-constrained settings.

Supplementary Materials: The following supporting information can be downloaded at: https://www.mdpi.com/article/doi/s1, Figure S1: title; Table S1: title; Video S1: title.

Author Contributions: Conceptualization, X.X. and Y.Y.; methodology, X.X.; software, X.X.; validation, X.X., Y.Y. and Z.Z.; formal analysis, X.X.; investigation, X.X.; resources, X.X.; data curation, X.X.; writing—original draft preparation, X.X.; writing—review and editing, X.X.; visualization, X.X.; supervision, X.X.; project administration, X.X.; funding acquisition, Y.Y. All authors have read and agreed to the published version of the manuscript."

Funding: This research received no external funding

Institutional Review Board Statement: In

Informed Consent Statement: Informed consent was obtained from all subjects involved in the study.

Data Availability Statement: The data presented in this study are available on request from the corresponding author.

Acknowledgments: We would like to express our gratitude to the patient involved for his support during the testing phases.

Conflicts of Interest: The authors declare no conflicts of interest.

Abbreviations

The following abbreviations are used in this manuscript:

MDPI	Multidisciplinary Digital Publishing Institute
DOAJ	Directory of open access journals
TLA	Three letter acronym
LD	Linear dichroism

References

1 A. Imran, B. Beigzadeh, and M. R. Haghjoo, "A new passive transfemoral prosthesis mechanism based on 3R36 knee and ESAR foot providing walking and squatting," *Theoretical and Applied Mechanics Letters*, vol. 13, no. 5, Sep. 2023, doi: 10.1016/j.taml.2023.100476.

[2] H. Fu *et al.*, "A novel prosthetic knee joint with a parallel spring and damping mechanism," *Int. J. Adv. Robot. Syst.*, vol. 13, no. 4, Aug. 2016, doi: 10.1177/1729881416658174.

[3] T. S. Anand and S. Sujatha, "A method for performance comparison of polycentric knees and its application to the design of a knee for developing countries," *Prosthet. Orthot. Int.*, vol. 41, no. 4, pp. 402–411, Aug. 2017, doi: 10.1177/0309364616652017.

[4] L. Galey, G. Beckmann, E. Ramos, F. A. Rangel, and R. V. Gonzalez, "Optimization of a Cost-Constrained, Hydraulic Knee Prosthesis Using a Kinematic Analysis Model," *Biomechanics (Switzerland)*, vol. 3, no. 4, pp. 493–510, Dec. 2023, doi: 10.3390/biomechanics3040040.

[5] M. G. Bernal-Torres, H. I. Medellín-Castillo, and J. C. Arellano-González, "Design and Control of a New Biomimetic Transfemoral Knee Prosthesis Using an Echo-Control Scheme," *J. Healthc. Eng.*, vol. 2018, 2018, doi: 10.1155/2018/8783642.

[6] M. Murabayashi, T. Mitani, and K. Inoue, "Development and Evaluation of a Passive Mechanism for a Transfemoral Prosthetic Knee That Prevents Falls during Running Stance," *Prosthesis*, vol. 4, no. 2, pp. 172–183, Jun. 2022, doi: 10.3390/prosthesis4020018.

[7] W. Liang *et al.*, "Mechanisms and component design of prosthetic knees: A review from a biomechanical function perspective," Sep. 15, 2022, *Frontiers Media S.A.* doi: 10.3389/fbioe.2022.950110.

[8] S. Phoengsongkhro, P. Tangpornprasert, P. Yotnuengnit, M. Samala, and C. Virulsri, "Development of four-bar polycentric knee joint with stance-phase knee flexion," *Sci. Rep.*, vol. 13, no. 1, Dec. 2023, doi: 10.1038/s41598-023-49879-4.

[9] R. K. Mohanty, R. C. Mohanty, and S. K. Sabut, "Finite element analysis and experimental validation of polycentric prosthetic knee," *Mater. Today Proc.*, vol. 63, pp. 207–214, Jan. 2022, doi: 10.1016/j.matpr.2022.02.509.

[10] V. Jaiswal and S. Kanagaraj, "Structural testing of a passive polycentric knee joint with advanced functionalities designed and developed for patient-specific fitting," *Journal of the Brazilian Society of Mechanical Sciences and Engineering*, vol. 46, no. 4, Apr. 2024, doi: 10.1007/s40430-024-04837-7.

[11] S. Phanphet, S. Dechjarern, and S. Jomjanyong, "Above-knee prosthesis design based on fatigue life using finite element method and design of experiment," *Med. Eng. Phys.*, vol. 43, pp. 86–91, May 2017, doi: 10.1016/j.medengphy.2017.01.001.

[12] R. K. Mohanty, R. C. Mohanty, and S. K. Sabut, "Design and analysis of polycentric prosthetic knee with enhanced kinematics and stability," Aug. 24, 2022. doi: 10.21203/rs.3.rs-1961964/v1.

[13] S. Lapapong, S. Sucharitpwatskul, N. Pitaksapsin, C. Srisurangkul, S. Lerspalungsanti, and R. Naewngerndee, "Finite element modeling and validation of a four-bar linkage prosthetic knee under static and cyclic strength tests," in *i-CREATe 2013 - International Convention on Rehabilitation Engineering and Assistive Technology, in Conjunction with SENDEX 2013*, 2013. doi: 10.3402/jartt.v2.23211.

[14] C. Ayala, F. Valencia, B. Gámez, H. Salazar, and D. Ojeda, "Personalized External Knee Prosthesis Design Using Instantaneous Center of Rotation for Improved Gait Emulation," *Prosthesis*, vol. 7, no. 6, Dec. 2025, doi: 10.3390/prosthesis7060163.

[15] Q. Zuo, J. Zhao, X. Mei, F. Yi, and G. Hu, "Design and trajectory tracking control of a magnetorheological prosthetic knee joint," *Applied Sciences (Switzerland)*, vol. 11, no. 18, Sep. 2021, doi: 10.3390/app11188305.

[16] D. A. Türk, H. Einarsson, C. Lecomte, and M. Meboldt, "Design and manufacturing of high-performance prostheses with additive manufacturing and fiber-reinforced polymers," *Production Engineering*, vol. 12, no. 2, pp. 203–213, Apr. 2018, doi: 10.1007/s11740-018-0799-y.

[17] J. F. Soriano, J. E. Rodríguez, and L. A. Valencia, "Performance comparison and design of an optimal polycentric knee mechanism," *Journal of the Brazilian Society of Mechanical Sciences and Engineering*, vol. 42, no. 5, May 2020, doi: 10.1007/s40430-020-02313-6.

[18] V. N. M. Arelekatti, N. T. Petelina, W. B. Johnson, M. J. Major, and A. G. Winter, "Design of a Four-Bar Latch Mechanism and a Shear-Based Rotary Viscous Damper for Single-Axis Prosthetic Knees," *J. Mech. Robot.*, vol. 14, no. 3, Jun. 2022, doi: 10.1115/1.4052804.

[19] L. Xu, D. H. Wang, Q. Fu, G. Yuan, and L. Z. Hu, "A novel four-bar linkage prosthetic knee based on magnetorheological effect: Principle, structure, simulation and control," *Smart Mater. Struct.*, vol. 25, no. 11, Oct. 2016, doi: 10.1088/0964-1726/25/11/115007.

[20] Z. Zhang, H. Yu, W. Cao, X. Wang, Q. Meng, and C. Chen, "Design of a semi-active prosthetic knee for transfemoral amputees: Gait symmetry research by simulation," *Applied Sciences (Switzerland)*, vol. 11, no. 12, Jun. 2021, doi: 10.3390/app11125328.

[21] W. Cao, H. Yu, W. Chen, Q. Meng, and C. Chen, "Design and Evaluation of a Novel Microprocessor-Controlled Prosthetic Knee," *IEEE Access*, vol. 7, pp. 178553–178562, 2019, doi: 10.1109/ACCESS.2019.2957823.

[22] X. Wang *et al.*, "Design and Validation of a Polycentric Hybrid Knee Prosthesis with Electromagnet-Controlled Mode Transition," *IEEE Robot. Autom. Lett.*, vol. 7, no. 4, pp. 10502–10509, Oct. 2022, doi: 10.1109/LRA.2022.3193462.

[23] N. A. Hamzaid, N. Azuan, A. Osman, and A. M. El-Sayed, "Modelling and Control of a Linear Actuated Transfemoral Knee Joint in Basic Daily Movements," *Applied Mathematics& Information Sciences An International Journal*, vol. 7, no. 1, pp. 1–11, 2014, doi: 10.12785/amis.

[24] S. M. J. Haider, A. M. Takhakh, M. Al-Waily, and Y. Saadi, "Simulation of gait cycle in sagittal plane for above-knee prosthesis," in *AIP Conference Proceedings*, American Institute of Physics Inc., Jan. 2022. doi: 10.1063/5.0066819.

[25] S. Ding, X. Ouyang, B. Fan, H. Yang, and G. Gong, "Dynamic simulation of a hydraulic exoskeleton robot based on virtual prototyping," in *IEEE/ASME International Conference on Advanced Intelligent Mechatronics, AIM*, Institute of Electrical and Electronics Engineers Inc., Sep. 2016, pp. 1479–1484. doi: 10.1109/AIM.2016.7576979.

[26] H. Wu, T. Jia, N. Li, J. Wu, and L. Yan, "Study on the control algorithm for lower limb exoskeleton

based on ADAMS/Simulink co-simulation," *Journal of Vibroengineering*, vol. 19, no. 4, pp. 2976–2986, 2017, doi: 10.21595/jve.2017.17303.

[27] Q. Su, Z. Pei, Z. Tang, and Q. Liang, "Design and Analysis of a Lower Limb Loadbearing Exoskeleton," *Actuators*, vol. 11, no. 10, Oct. 2022, doi: 10.3390/act11100285.

[28] L. Pan, C. He, and Q. Li, "Structural Static Characteristic Analysis of Lower Limb Exoskeleton Based on Finite Element Modeling," 2015.

[29] J. S. Salgado Manrique and C. Cifuentes-De la Portilla, "Exploring Opportunities for Advancements in Lower Limb Socket Fabrication and Testing: A Review," Sep. 01, 2025, *Multidisciplinary Digital Publishing Institute (MDPI)*. doi: 10.3390/biomechanics5030064.

[1]

[30] F. Gariboldi, M. Scapinello, N. Petrone, G. L. Migliore, G. Teti, and A. G. Cutti, "Static strength of lower-limb prosthetic sockets: An exploratory study on the influence of stratigraphy, distal adapter and lamination resin," *Med. Eng. Phys.*, vol. 114, Apr. 2023, doi: 10.1016/j.medengphy.2023.103970.

[31] G. R. Gubbala and R. Inala, "Design and development of patient-specific prosthetic socket for lower limb amputation," *Material Science, Engineering and Applications*, vol. 1, no. 2, pp. 32–42, Dec. 2021, doi: 10.21595/msea.2021.22012.

[32] E. Saynes-Vazquez and E. Lugo González, "Optimization of 4 and 6 Link Planar Mechanisms for the Development of a Transfemoral Prosthesis Prototype," Huajuapan, Apr. 2022.

[33] J. Narayan, M. Abbas, and S. K. Dwivedy, "Robust adaptive backstepping control for a lower-limb exoskeleton system with model uncertainties and external disturbances," *Automatika*, vol. 64, no. 1, pp. 145–161, 2023, doi: 10.1080/00051144.2022.2119498.

M. Baumann *et al.*, "The relationship between residual limb health, motion within the socket, and prosthetic suspension," Apr. 01, 2023, *John Wiley and Sons Inc*. doi: 10.1002/pmrj.12899.